COMMUNICATION

Bioinspired Bifunctional Catalyst: Amphiphilic Organometallic Catalyst for Ring-Closing Metathesis Forming Liquid Droplets in Aqueous Media†

Received 00th January 20xx,
Accepted 00th January 20xx

DOI: 10.1039/x0xx00000x

Miki Mori,[a] Hiroka Sugai,[b] Kohei Sato,[a, ‡] Asuki Okada,[c] Takashi Matsuo,[c] and Kazushi Kinbara* [a, b]

Inspired by phase-separated biopolymers with enzymatic activity, we developed an amphiphilic catalyst consisting of alternating hydrophilic oligo(ethylene glycol) and hydrophobic aromatic units bearing a Hoveyda-Grubbs catalyst center (MAHGII). MAHGII served as both a droplet-forming scaffold and a catalyst for ring-closing metathesis reactions, providing a new biomimetic system that promotes organic reactions in an aqueous environment.

Creating life-like functions from abiotic molecules is a crucial issue for constructively understanding complicated living systems[1,2] or developing bioinspired technologies.[3,4] Among various life-like functions,[5] compartmentalization and chemical reactions therein are especially fundamental principles that underlie the spatiotemporal regulation of molecular processes in life.[6,7] Encouraged by recent increasing attention on membrane-less organelles in the cells,[8–10] phase-separated condensates of biopolymers have become widely recognized as one of bioinspired compartments. Many *in vitro* experiments have demonstrated that their liquid-like nature allows selective incorporation/exclusion between droplets and surrounding solutions,[11–13] and highly condensed environments in droplets contribute to an acceleration of chemical reactions.[14–16] Recent studies have also reported that several proteins with enzymatic activity, such as the RNA helicase LAF-1[17] and Ddx4,[18] double as a phase-separated scaffold, showing the sophisticated catalytic reaction field in nature.

In this context, although there have been numerous instances of phase-separated droplets composed of synthetic polymers exhibiting low critical solution temperatures (LCST),[19] the potential of synthetic catalysts within such droplets remains unexplored, despite the various strategies that have been proposed for using water as a solvent in catalytic organic reactions,[20,21] including the development of water-soluble homogeneous precatalysts,[22–27] on-water synthesis,[28,29] micellar catalysis,[30–37] utilization of organic cosolvents,[33,38,39] and bio-catalysis.[40,41] In particular, a single synthetic compound, that can act as both a catalyst and a reaction field like the phase-separated droplets in an aqueous environment, has not yet been achieved.

Herein, we introduce a new concept of artificial catalytic reaction field in an aqueous environment: organometallic reactions by a liquid droplet-forming transition metal catalyst. Inspired by a natural catalytic reaction field consisting of a rigid enzymatic domain and flexible intrinsically disordered regions, such as LAF-1[17] and Ddx4,[18] we designed a compound with a rigid transition metal catalytic unit and flexible hydrophilic polymer moieties. We synthesized a multiblock amphiphilic Hoveyda-Grubbs 2nd generation catalyst (**MAHGII**, Fig. 1) which is composed of hydrophilic octa(ethylene glycol) chains and hydrophobic aromatic units with a catalytic moiety at the center. The amphiphilic poly(ethylene glycol) (PEG)-based structure was adopted from its flexible conformation, and also from its droplet-forming property in aqueous media demonstrated in our previous report.[42] Hoveyda-Grubbs 2nd generation catalysts are known as air- and water-tolerant catalysts for olefin metathesis reactions,[43,44] which could be an ideal model in this study.

The multiblock *N*-heterocyclic carbene (NHC) ligand precursor was synthesized following the previously reported procedures by our group.[45] The complexation of the NHC ligand precursor with Grubbs 1st generation catalyst was carried out under basic conditions, followed by ligand exchange with 2-isopropoxystyrene to afford the Hoveyda-type 2nd generation catalytic unit. All the newly synthesized compounds were

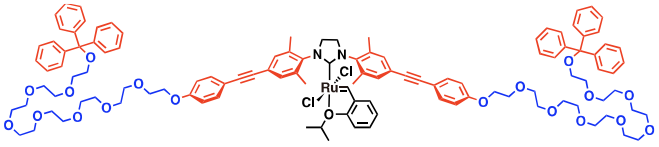

Fig. 1 Molecular structure of **MAHGII**. Red, blue, and black indicate the hydrophobic, hydrophilic, and catalytic units, respectively.

[a] *School of Life Science and Technology, Tokyo Institute of Technology, 4259 Nagatsuta-cho, Midori-ku, Yokohama 226-8501, Japan. E-mail: kinbara.k.aa@m.titech.ac.jp*
[b] *Research Center for Autonomous Systems Materialogy (ASMat), Institute of Innovative Research, Tokyo Institute of Technology, 4259 Nagatsuta-cho, Midori-ku, Yokohama 226-8501, Japan*
[c] *Division of Materials Science, Nara Institute of Science and Technology, 8916-5 Takayama-cho, Ikoma 630-0192, Japan*
†Electronic Supplementary Information (ESI) available: Details of synthesis, characterization, and experimental procedures. See DOI: 10.1039/x0xx00000x
‡Present address: Department of Chemistry, School of Science, Kwansei Gakuin University, 1 Gakuen Uegahara, Sanda-shi, Hyogo 669-1330, Japan

Please do not adjust margins

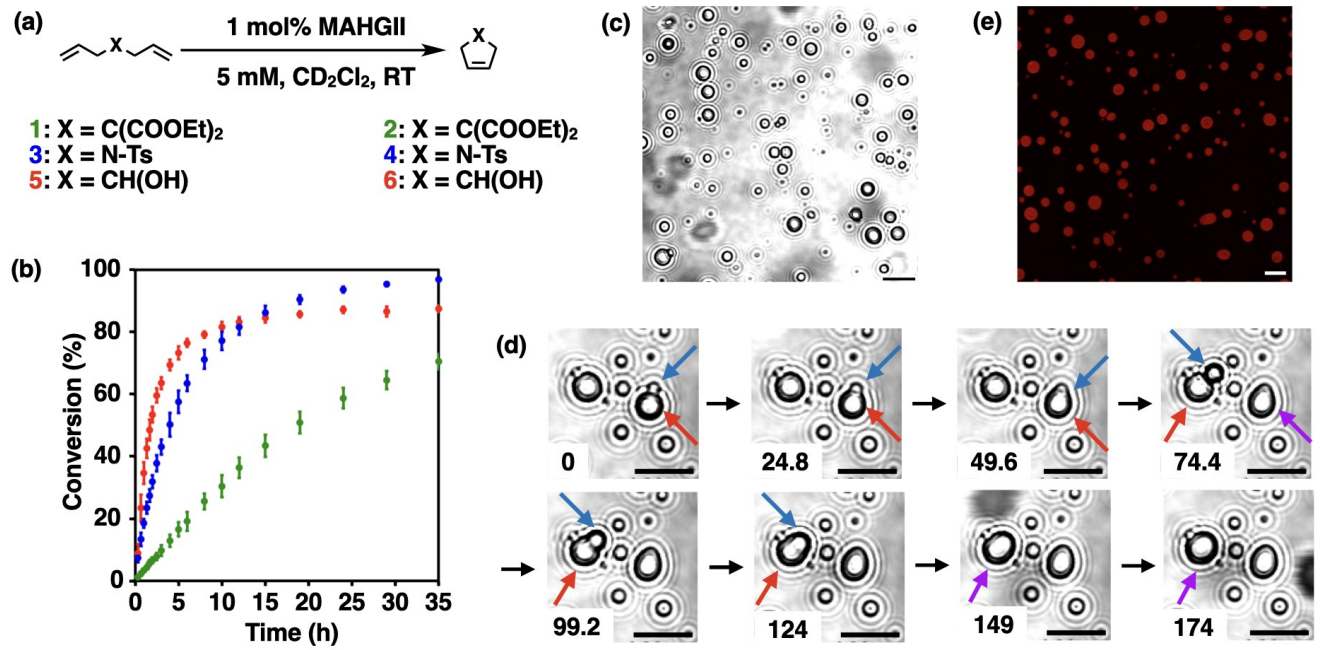

Fig. 2 (a) Reaction conditions for RCM reactions catalyzed by **MAHGII** and structures of substrates and products. (b) Time versus conversion profiles of RCM reactions of **1** (green), **3** (blue) and **5** (red) catalyzed by **MAHGII** in CD_2Cl_2. All reactions were performed in triplicate and the error bars represent the standard deviation. (c) Phase-contrast micrographs of **MAHGII** droplets. [**MAHGII**] = 200 μM in 100 mM KCl aq. with 1 v/v% DMF. (d) Timelapse phase-contrast micrographs tracking the fusion events of **MAHGII** liquid droplets. The pair of droplets indicated by the blue and red arrows fused into a single droplet indicated by the purple arrow. Numbers on the left bottom of each images represent the time points in seconds. [**MAHGII**] = 200 μM in 100 mM KCl aq. with 1 v/v% DMF. (e) Confocal laser scanning microscopic image representing the accumulation of hydrophobic Nile Red into **MAHGII** droplets. [**MAHGII**] = 200 μM, [Nile Red] = 10 μM in 100 mM KCl aq. with 1 v/v% DMF (λ_{ex} = 559 nm, λ_{obsd} = 612 nm). Scale bars: 5 μm.

characterized by ^{1}H and ^{13}C NMR spectroscopy and high-resolution ESI-TOF-MS spectrometry (Fig. S1–S9, ESI).

First, we investigated the catalytic activity of **MAHGII** in an organic solution. Ring-closing metathesis (RCM) reactions were carried out in CD_2Cl_2 with three substrates: diethyl diallylmalonate (**1**), *N*,*N*-diallyl-4-methylbenzenesulfonamide (**3**) and 1,6-heptadien-4-ol (**5**), which gave the cyclized products **2**, **4**, and **6**, respectively (Fig. 2a). Reactions were performed at room temperature under open air at a substrate concentration of 5 mM with 1 mol% catalyst loading. The conversions were calculated based on ^{1}H NMR spectroscopy over 35 h. The RCM reaction of **1** proceeded slowest and gave the lowest conversion of 70% among the three substrates examined (Fig. 2b, green dots). In contrast, the reaction proceeded fastest for **5**, which reached to its plateau around 15 h with the conversion of 86% (Fig. 2b, red dots). The RCM of **3** was initiated slower compared to **5**, however gave the highest conversion of 96 % after 35 h (Fig. 2b, blue dots). These trends of the kinetic profile followed those observed for the commercially available Hoveyda-Grubbs 2nd generation catalyst (**HGII**) under the same reaction conditions (Fig. S10, ESI). Although the NHC unit includes ethyne units, the ene-yne-type metathesis product was not observed in each case.

Having confirmed that **MAHGII** with the amphiphilic moieties kept the similar catalytic activity with **HGII**, we then examined the capability of **MAHGII** to form liquid droplets in aqueous environments. A DMF solution of **MAHGII** was added to a 100 mM KCl aq. under stirring at room temperature. Here, a 100 mM KCl aq. was chosen as a solvent to stabilize the catalytic Ru center, where the equilibrium of the Ru complex is shifted to the chloride-coordinated catalytically active state rather than the hydroxide-coordinated inactive state.[46,47] As shown in Fig. 2c, micrometer-sized spherical droplets were observed by phase contrast microscopy. Importantly, these droplets could coalesce over time (Fig. 2d), showing the liquid-like nature of the **MAHGII** droplets. In addition, the capability of the **MAHGII** droplets to accumulate other molecules within themselves was investigated by using Nile Red, a hydrophobic dye. Confocal laser scanning microscopy (CLSM) showed the localization of the red emission due to Nile Red within the **MAHGII** droplets (Fig. 2e). The gray values of the Nile Red emission across the droplet showed the mostly constant values (Fig. S11, ESI), indicating the uniform distribution of Nile Red in the droplet. These results suggested that the **MAHGII** droplets could accumulate the hydrophobic molecules.

Since the **MAHGII** droplets were shown to act as hydrophobic containers in an aqueous environment, the catalytic activity of **MAHGII** droplets was investigated for the RCM reaction. **5** was chosen as a model substrate because it allows direct measurement of the reaction progress by ^{1}H NMR spectroscopy in aqueous environments. The reaction mixtures were prepared by dispersing the DMF solution of **MAHGII** in 100 mM KCl D_2O solution, followed by the addition of DMF solution of **5**, so that the final concentrations of **MAHGII** and **5** were 200 μM and 5 mM, respectively. Note that **5** did not disrupt the **MAHGII** droplets under these concentrations (Fig. S12, ESI). The dynamic light scattering (DLS) measurement (Fig. S13, ESI) also indicated that **5** formed tiny droplets with hydrodynamic

This journal is © The Royal Society of Chemistry 20xx

Please do not adjust margins

Please do not adjust margins

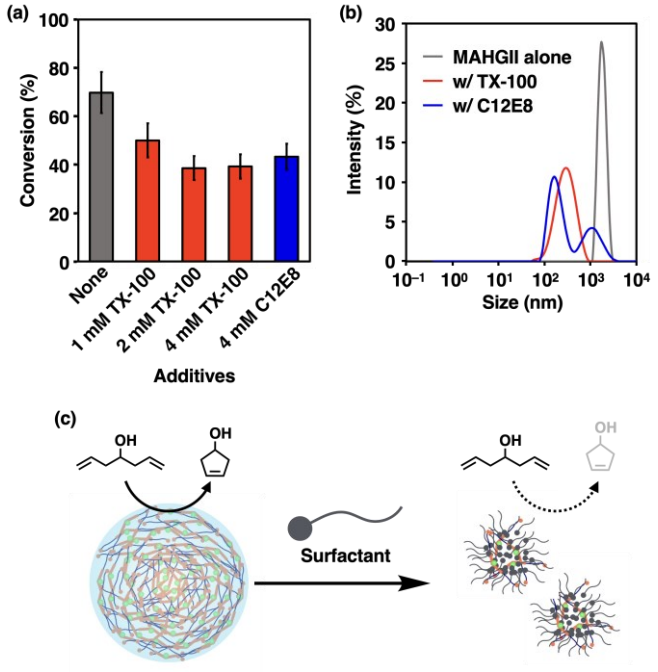

Fig. 3 (a) Comparison of RCM conversions of **5** catalyzed by **MAHGII** in the presence and absence of surfactants in 100 mM KCl D_2O. [**MAHGII**] = 200 µM, [**5**] = 5 mM, at 50 °C for 4 h under open air without stirring. The reactions were carried out at least twice and error bars represent the standard deviation. (b) DLS profile of **MAHGII** alone (gray) and in the presence of TX-100 (red) or C12E8 (blue). [**MAHGII**] = 200 µM, [TX-100] = [C12E8] = 4 mM in 100 mM KCl aq., 20 °C. (c) Schematic illustration of surfactant-induced droplet disruption that leads to deactivation of catalysis by **MAHGII** droplets.

diameter D_H of 440 nm, which disappeared in the presence of **MAHGII**, while the size of the **MAHGII** droplets (D_H = 1.8 µm) remained unchanged. This result indicated that **MAHGII** droplets accommodated **5**. Then, the reaction mixtures were heated at 50 °C for 4 h under open air without stirring, which was cooled down to room temperature for ^{1}H NMR measurement to evaluate the conversion.[48] The conversion of the RCM reaction catalyzed by **MAHGII** droplets reached to 70% (Fig. 3a, gray bar) whereas that by the commercially available **HGII** under the same conditions was only 16% (Fig. S14, ESI). Since the RCM reaction carried out in an organic solution (in $CDCl_3$) under the same reaction conditions proceeded quantitatively (Fig. S15, ESI), it is noteworthy that **MAHGII** maintained the high catalytic activity compared to **HGII** in an aqueous media.

Furthermore, we examined the importance of the droplet formation on the catalytic activity. Here, we chose two neutral surfactants, Triton X-100 (TX-100) and octa(ethylene glycol) monododecyl ether (C12E8). Prior to performing the RCM reaction of **5** in the presence of these surfactants, we confirmed the prevention of the droplet formation using DLS. **MAHGII** alone gave a monodisperse size distribution with D_H of 1.8 µm (Fig. 3b, gray line). In contrast, **MAHGII** in the presence of TX-100 and C12E8 gave monodisperse size distribution with D_H of 315 nm and polydisperse size distribution with D_H of 193 nm and 1.2 µm, respectively (Fig. 3b, red and blue lines). These results suggested that the **MAHGII** droplets were disrupted in the presence of surfactants. Then we carried out the RCM reaction in the presence of various concentrations of surfactants, while those of **5** and **MAHGII** were fixed to 5 mM and 200 µM, respectively. In the presence of 1 mM TX-100, the conversion dropped to 50%. Upon increasing the TX-100 concentration to 2 mM and 4 mM, the drop in the conversion had likely reached to a plateau, giving the conversion of 39% for both concentrations (Fig. 3a, red bars). Similarly, the conversion dropped to 43% in the presence of 4 mM C12E8 (Fig. 3a, blue bars). In sharp contrast to these results, the catalytic activity of commercially available **HGII** enhanced to 50–58% in the presence of the surfactants (Fig. S14, ESI) while those without any surfactant reached only 16% as mentioned above. Altogether, the disruption of the **MAHGII** droplets by the surfactants led to the decrease of the catalytic activity of **MAHGII**, suggesting that the droplets were indeed providing efficient environments for the RCM reaction in the aqueous media (Fig. 3c).

In conclusion, inspired by the phase-separated biopolymers in nature, we designed and synthesized a multiblock amphiphilic Hoveyda-Grubbs 2nd generation catalyst (**MAHGII**), bearing both rigid catalytic active and flexible droplet-inducing moieties. NMR spectroscopic and microscopic experiments demonstrated that the **MAHGII** droplets successfully catalyzed the RCM reactions in aqueous environments. In some cellular systems, the acceleration of reactions induced by the colocalization of the catalyst with its substrate within the droplets has been observed. Examples include the mRNA processing reaction within the histone locus body[49] and the pre-mRNA splicing reaction within Cajal bodies in zebrafish.[50] **MAHGII** successfully demonstrated the expansion of similar systems to an abiotic catalytic reaction, specifically the RCM reaction. Furthermore, the use of water as a solvent in organic synthesis has massive advantages over the organic solvents not only for biological applications but also for green chemistry.[51,52] Therefore, we believe that this study could potentially be recognized as one of the new concepts for biomimetic organometallic catalysis in an aqueous environment, which contributes to develop the environmental-friendly organic synthetic procedures.

Miki Mori: investigation; funding acquisition; writing – original draft. Hiroka Sugai: investigation; writing – original draft; writing – review & editing. Kohei Sato: Project administration; funding acquisition; writing – review & editing. Asuki Okada: investigation. Takashi Matsuo: resources; writing – review & editing. Kazushi Kinbara: conceptualization; supervision; resources; funding acquisition; project administration; writing – review & editing.

The authors thank Suzukakedai Materials Analysis Division, Open Facility, Tokyo Institute of Technology for ESI-TOF-MS spectrometry and NMR spectroscopy, and Prof. M. Takinoue, Tokyo Institute of Technology, for CLSM. This work was supported by Grant-in-Aid for Scientific Research on Innovative Areas "Molecular Engine" (18H05418, 18H05419, and 23H05418 to KK), Grant-in-Aid for Challenging Research (Pioneering) (23K17363 to KK), Grant-in-Aid for Scientific Research (B) (23H02080 to KS), Grant-in-Aid for Challenging Research (Exploratory) (23K17973 to KS), Grant-in-Aid for Transformative Research Areas "Molecular Cybernetics"

Please do not adjust margins

Please do not adjust margins

(23H04408 to KS), Grant-in-Aid for JSPS Fellows (JP22J14625 to MM), and JST SPRING (JPMJSP2106 to MM). MM also thanks the Leave a Nest Grant in·cube award.

Conflicts of interest

There are no conflicts to declare.

Notes and references

1 S. Mann, *Acc. Chem. Res.*, 2012, **45**, 2131–2141.
2 W. Jiang, Z. Wu, Z. Gao, M. Wan, M. Zhou, C. Mao and J. Shen, *ACS Nano*, 2022, **16**, 15705–15733.
3 A. Levin, T. A. Hakala, L. Schnaider, G. J. L. Bernardes, E. Gazit and T. P. J. Knowles, *Nat. Rev. Chem.*, 2020, **4**, 615–634.
4 X. Wang, X. Liu and X. Huang, *Adv. Mater.*, 2020, **32**, e2001436.
5 N. A. Yewdall, A. F. Mason and J. C. M. van Hest, *Interface Focus*, 2018, **8**, 20180023.
6 M. J. York-Duran, M. Godoy-Gallardo, C. Labay, A. J. Urquhart, T. L. Andresen and L. Hosta-Rigau, *Colloids Surf. B Biointerfaces*, 2017, **152**, 199–213.
7 P.-A. Monnard and P. Walde, *Life*, 2015, **5**, 1239–1263.
8 A. S. Lyon, W. B. Peeples and M. K. Rosen, *Nat. Rev. Mol. Cell Biol.*, 2021, **22**, 215–235.
9 D. L. J. Lafontaine, J. A. Riback, R. Bascetin and C. P. Brangwynne, *Nat. Rev. Mol. Cell Biol.*, 2021, **22**, 165–182.
10 S. Alberti and A. A. Hyman, *Nat. Rev. Mol. Cell Biol.*, 2021, **22**, 196–213.
11 T.-Y. Dora Tang, C. Rohaida Che Hak, A. J. Thompson, M. K. Kuimova, D. S. Williams, A. W. Perriman and S. Mann, *Nat. Chem.*, 2014, **6**, 527–533.
12 T. Lu and E. Spruijt, *J. Am. Chem. Soc.*, 2020, **142**, 2905–2914.
13 I. A. Klein, A. Boija, L. K. Afeyan, S. W. Hawken, M. Fan, A. Dall'Agnese, O. Oksuz, J. E. Henninger, K. Shrinivas, B. R. Sabari, I. Sagi, V. E. Clark, J. M. Platt, M. Kar, P. M. McCall, A. V. Zamudio, J. C. Manteiga, E. L. Coffey, C. H. Li, N. M. Hannett, Y. E. Guo, T.-M. Decker, T. I. Lee, T. Zhang, J.-K. Weng, D. J. Taatjes, A. Chakraborty, P. A. Sharp, Y. T. Chang, A. A. Hyman, N. S. Gray and R. A. Young, *Science*, 2020, **368**, 1386–1392.
14 R. R. Poudyal, R. M. Guth-Metzler, A. J. Veenis, E. A. Frankel, C. D. Keating and P. C. Bevilacqua, *Nat. Commun.*, 2019, **10**, 490.
15 R. R. Poudyal, C. D. Keating and P. C. Bevilacqua, *ACS Chem. Biol.*, 2019, **14**, 1243–1248.
16 M. Abbas, W. P. Lipiński, K. K. Nakashima, W. T. S. Huck and E. Spruijt, *Nat. Chem.*, 2021, **13**, 1046–1054.
17 S. Elbaum-Garfinkle, Y. Kim, K. Szczepaniak, C. C.-H. Chen, C. R. Eckmann, S. Myong and C. P. Brangwynne, *Proc. Natl. Acad. Sci. U. S. A.*, 2015, **112**, 7189–7194.
18 T. J. Nott, E. Petsalaki, P. Farber, D. Jervis, E. Fussner, A. Plochowietz, T. D. Craggs, D. P. Bazett-Jones, T. Pawson, J. D. Forman-Kay and A. J. Baldwin, *Mol. Cell*, 2015, **57**, 936–947.
19 Y. Yuan, K. Raheja, N. B. Milbrandt, S. Beilharz, S. Tene, S. Oshabaheebwa, U. A. Gurkan, A. C. S. Samia and M. Karayilan, *RSC Appl. Polym.*, 2023, **1**, 158–189.
20 U. M. Lindström, *Chem. Rev.*, 2002, **102**, 2751–2772.
21 C.-J. Li, *Chem. Rev.*, 2005, **105**, 3095–3165.
22 T. J. Ahmed, L. N. Zakharov and D. R. Tyler, *Organometallics*, 2007, **26**, 5179–5187.
23 J. P. Jordan and R. H. Grubbs, *Angew. Chem. Int. Ed.*, 2007, **46**, 5152–5155.
24 K. Skowerski, G. Szczepaniak, C. Wierzbicka, Ł. Gułajski, M. Bieniek and K. Grela, *Catal. Sci. Technol.*, 2012, **2**, 2424–2427.
25 Z. J. Wang, W. Roy Jackson and A. J. Robinson, *Green Chem.*, 2015, **17**, 3407–3414.
26 M. Finn, J. A. Ridenour, J. Heltzel, C. Cahill and A. Voutchkova-Kostal, *Organometallics*, 2018, **37**, 1400–1409.
27 I. Nicolas, P. L. Maux and G. Simonneaux, *Tetrahedron Lett.*, 2008, **49**, 5793–5795.
28 S. Narayan, J. Muldoon, M. G. Finn, V. V. Fokin, H. C. Kolb and K. B. Sharpless, *Angew. Chem. Int. Ed.*, 2005, **44**, 3275–3279.
29 A. Chanda and V. V. Fokin, *Chem. Rev.*, 2009, **109**, 725–748.
30 T. Dwars, E. Paetzold and G. Oehme, *Angew. Chem. Int. Ed.*, 2005, **44**, 7174–7199.
31 B. H. Lipshutz, G. T. Aguinaldo, S. Ghorai and K. Voigtritter, *Org. Lett.*, 2008, **10**, 1325–1328.
32 G. La Sorella, G. Strukul and A. Scarso, *Green Chem.*, 2015, **17**, 644–683.
33 C. M. Gabriel, N. R. Lee, F. Bigorne, P. Klumphu, M. Parmentier, F. Gallou and B. H. Lipshutz, *Org. Lett.*, 2017, **19**, 194–197.
34 B. H. Lipshutz, S. Ghorai and M. Cortes-Clerget, *Chem. Eur. J.*, 2018, **24**, 6672–6695.
35 M. Cortes-Clerget, N. Akporji, J. Zhou, F. Gao, P. Guo, M. Parmentier, F. Gallou, J.-Y. Berthon and B. H. Lipshutz, *Nat. Commun.*, 2019, **10**, 2169.
36 B. H. Lipshutz and S. Ghorai, *Org. Lett.*, 2009, **11**, 705–708.
37 B. H. Lipshutz and S. Ghorai, *Tetrahedron*, 2010, **66**, 1057–1063.
38 S. J. Connon, M. Rivard, M. Zaja and S. Blechert, *Adv. Synth. Catal.*, 2003, **345**, 572–575.
39 R. P. Megens and G. Roelfes, *Org. Biomol. Chem.*, 2010, **8**, 1387–1393.
40 T. K. Hyster, L. Knörr, T. R. Ward and T. Rovis, *Science*, 2012, **338**, 500–503.
41 F. Schwizer, Y. Okamoto, T. Heinisch, Y. Gu, M. M. Pellizzoni, V. Lebrun, R. Reuter, V. Köhler, J. C. Lewis and T. R. Ward, *Chem. Rev.*, 2018, **118**, 142–231.
42 S. Kawasaki, T. Muraoka, H. Obara, T. Ishii, T. Hamada and K. Kinbara, *Chem. Asian J.*, 2014, **9**, 2778–2788.
43 M. Scholl, S. Ding, C. W. Lee and R. H. Grubbs, *Org. Lett.*, 1999, **1**, 953–956.
44 S. B. Garber, J. S. Kingsbury, B. L. Gray and A. H. Hoveyda, *J. Am. Chem. Soc.*, 2000, **122**, 8168–8179.
45 M. Mori, K. Sato, T. Ekimoto, S. Okumura, M. Ikeguchi, K. V. Tabata, H. Noji and K. Kinbara, *Chem. Asian J.*, 2021, **16**, 147–157.
46 T. Matsuo, T. Yoshida, A. Fujii, K. Kawahara and S. Hirota, *Organometallics*, 2013, **32**, 5313–5319.
47 J. C. Foster, M. C. Grocott, L. A. Arkinstall, S. Varlas, M. J. Redding, S. M. Grayson and R. K. O'Reilly, *J. Am. Chem. Soc.*, 2020, **142**, 13878–13885.
48 The real-time monitoring of the RCM reaction using ^{1}H NMR spectroscopy turned out to be difficult due to the heterogeneity of the reaction media.
49 D. C. Tatomer, E. Terzo, K. P. Curry, H. Salzler, I. Sabath, G. Zapotoczny, D. J. McKay, Z. Dominski, W. F. Marzluff and R. J. Duronio, *J. Cell Biol.*, 2016, **213**, 557–570.
50 M. Strzelecka, S. Trowitzsch, G. Weber, R. Lührmann, A. C. Oates and K. M. Neugebauer, *Nat. Struct. Mol. Biol.*, 2010, **17**, 403–409.
51 J. C. Jewett and C. R. Bertozzi, *Chem. Soc. Rev.*, 2010, **39**, 1272–1279.
52 M.-O. Simon and C.-J. Li, *Chem. Soc. Rev.*, 2012, **41**, 1415–1427.

 This journal is © The Royal Society of Chemistry 20xx

Please do not adjust margins